ISSN(Online) : 2319-8753
ISSN (Print) : 2347-6710

International Journal of Innovative Research in Science, Engineering and Technology

(An UGC Approved, High Impact Factor, Monthly, Peer Reviewed Journal) | Impact Factor: 7.089|

UGC Approval No: 48027

Vol. 6, Issue 4, April 2017

Special Effects of nanomorphology on the Performance of ZnO-based Schottky Diode Devices

Somnath Middya*

*Department of Physics, Bankim Sardar College, South 24 Parganas, West Bengal, India

INTRODUCTION: Over the last few years, major progress has been made in the development of inorganic semiconductor nanoparticles and their use in metal semiconductor Schottky diodes
to improve active materials and lower costs. Inorganic nanoparticles are the subject of board research due to their potential for optical, electrical and photovoltaic applications [1, 2]. Over the first years major progress has been made in the development of inorganic semiconductor and a particles and their use in metal semiconductors to improve activity and lower costs. Recent research on materials for organic light-emitting diodes (OLEDs) and solar cells has established that conjugating polymers with n-type inorganic nanoparticles can result in stable and high-performance materials [3]. Metal-semiconductor interactions have been effectively formed using a number of inorganic nanoparticles[4, 5]. ZnO is an n-type semiconductor material that is non-toxic among inorganic nanoparticles.

Metal semiconductor is frequently employed in Schottky diodes [6], light emitting diodes [7, 8], optical sensors [9], and solar cells [10] as a result of this characteristic. ZnO exhibits remarkable optical transparency and a relatively high exciton binding energy (60 meV) [11, 12]. It has been selected as one of the promising materials for the manufacture of inorganic semiconductor devices based on all these features [13, 14]. The device can function at low threshold voltages thanks to the substantial exciton binding energy of ZnO, which leads to steady exciton energy at high temperatures [15]. The modification of electron mobility caused by optimized shape is another significant characteristic of ZnO nanoparticles [16].By altering their morphology, nanomaterials with band gaps suitable for certain applications can be created. A quick change in the band gap results from absorption, which is dependent on the quality of the absorbing material's surface. The Burstein-Moss effect states that the geometrical evolution and doping concentrations of semiconductor nanoparticles push their absorption to higher energies [17]. All states near to the conduction band become filled as a result. At temperatures above room temperature, metals can be handled best by N-type semiconductor materials since they have a broader bandgap. ZnO, a conventional semiconductor, has a high bandgap that makes metal semiconductor Schottky diodes practical to use. The use of numerous metals, including Ag [18, 19], Au [20], Pd [21], and Pt [22, 23], in the development of ZnO-based Schottky barrier diodes has been reported. A Schottky barrier height of 0.6–0.8 eV and an ideality factor of 1.5 are typically produced by all of these materials [18–23].

There have been significant efforts put towards synthesizing ZnO nanoparticles with various structures. ZnO nanoparticles in the forms of flowers, prisms, rods, and snowflakes were demonstrated by Zhang et al.[24]. However, no research has yet been done on how morphology affects the physics of metal-semiconductor junctions in inorganic nano semiconductor materials. We add weight and thermal synthesis in this way.Continuous data characterization of nanoparticles is carried out. Investigations were done on the morphology-dependent optical band gap alterations and absorption of ZnO nanosemiconductor materials. Using artificial nanoparticles, Schottky diodes with an ITO/ZnO/Al structure were created. The I-V characteristic's rectification behaviour resembles that of a Schottky diode. This section investigates and summarises the primary variations in diode behaviour caused by ZnO nanoparticle shape.

ISSN(Online) : 2319-8753
ISSN (Print) : 2347-6710

International Journal of Innovative Research in Science, Engineering and Technology

(An UGC Approved, High Impact Factor, Monthly, Peer Reviewed Journal) | Impact Factor: 7.089|

UGC Approval No: 48027

Vol. 6, Issue 4, April 2017

Fundamental of Schottky diode:

If you place the n- type and p- type semiconductors very close together, you get a p-n junction, which is often used as a diode. When a metal surface is used to replace a p- type semiconductor, you get a Schottky barrier, also known as a Schottky diode. The major difference between Schottky barrier and p-n junction is generally lower junction voltage and reduce depreciation width in metal. Since the depletion layer in the metal is small and negligible, all depletion and potential difference occur in semiconductors.

Formation mechanism:

The Fermi level stops in the permissible band because metals are materials with overlapping valence bands. This translates into a very high electron density in current flow and a very high electron density at the Fermi level. Additionally, since the number of unoccupied States is equal, electrons can travel freely down the wire. Consequently the metal has a very high electrical conductivity. Electrons that are bound to a point are said to have negative energy, whereas unbound electrons are considered to be in a vacuum and have zero energy. The Fermi level E_f of a metal is approximately equal to the average energy of its most active electrons. These electrons can be released from the metal by adding some energy gradient. Metal working $ø_m$ is specific to the metal type.

Since the Fermi level is always inside the limit the extra energy that has to be released to free the electrons in a semiconductor is located roughly near the bottom of the material in figure 1. Electron affinity χs is also a special property. As we will see, the work function $ø_s$ of the semiconductor are still an important parameter. Bringing these two materials into contact requires a flat Fermi level and a constant vacuum. In a different process, these two changes are achieved by transferring some of the electronic components from the equipment to the other with a small process creating a dipole. Whose potential is equal to the Fermi level difference, $\mathbf{V_{bi} = ø_m - ø_s}$ **(**$\mathbf{I_{diff} = I_{drift}}$**).** It is necessary to have a flat Fermi level and a steady however in order to bring these two materials together. In an alternative method, these two modifications are made by moving a small number of electronic components from one piece of apparatus to another, producing a dipole whose potential is equal to the Fermi level difference, $\mathbf{V_{bi} = ø_m - ø_s}$ **(**$\mathbf{I_{diff} = I_{drift}}$**).**

In this case, the diffusion current is equal to opposing the current drifting from the dipole.

The diffusion current in this situation equals the opposite current that is drifting away from the dipole. A resulting barrier height $ø_b$, of a metal-semiconductor junction equals the difference between the metal work function, $ø_m$, and the electron affinity, χ_e, compare in Figure 2.

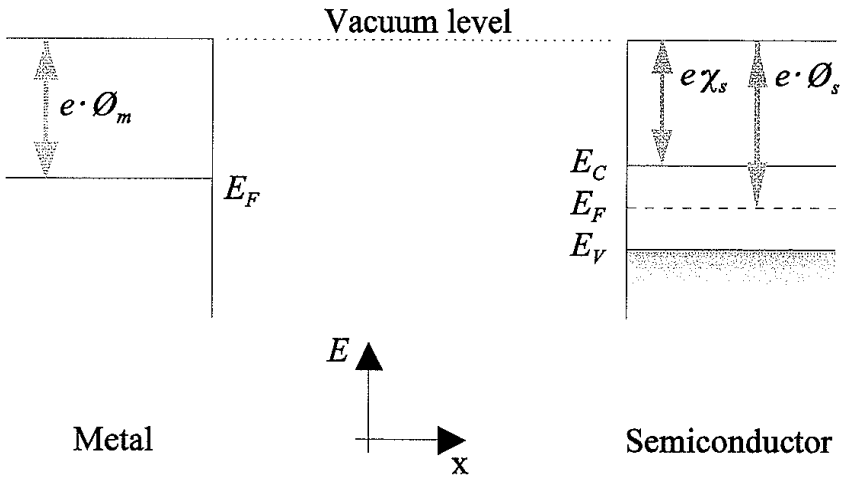

Figure 1: Flat band diagram of a metal and a semiconductor

ISSN(Online) : 2319-8753
ISSN (Print) : 2347-6710

International Journal of Innovative Research in Science, Engineering and Technology

(An UGC Approved, High Impact Factor, Monthly, Peer Reviewed Journal) | Impact Factor: 7.089|

UGC Approval No: 48027

Vol. 6, Issue 4, April 2017

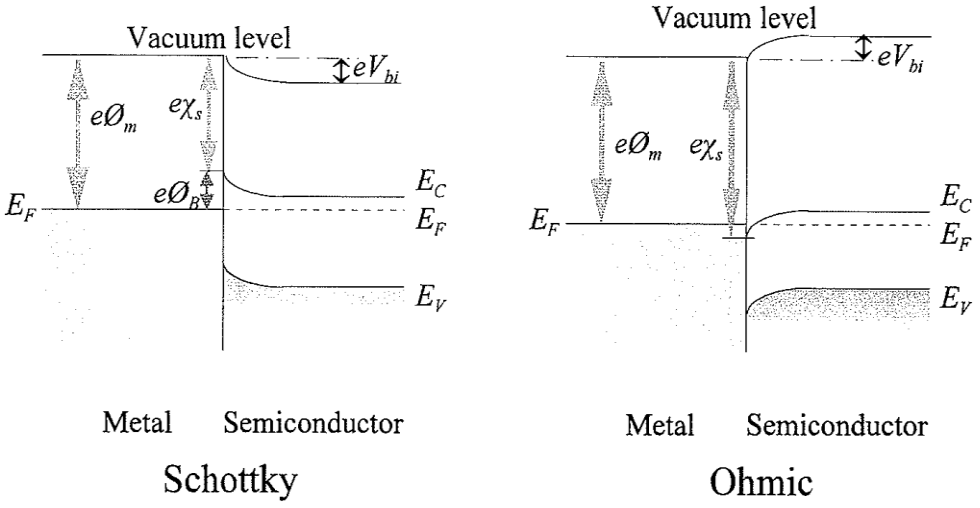

Figure 2: Band diagram of a metal to n-type semiconductor junction

Experimental:

1. **Synthesis of Rod and Sphere shaped ZnO:**

a. Experimental Reagents:

Anhydrous zinc acetate ($Zn(COOH)_2$:$2H_2O$),methanol, and AR gradesodium hydroxide (NaOH) particles were purchas ed from Merck for the synthesis of zinc oxide(ZnO)nanoparticles. Organic capping agents CTAB [cetyl tri methyl ammonium bromide] and PVP [Poly(vinyl pyrrolidone)] have been purchased from Sigma Aldrich.

b. Synthesis of ZnO nano rods:

To correct the morphology, the solvothermal growth process uses a capping agent for the roadlike ZnO structure; we use PVP as the capping agent. Typically,1mM(0.05g)Zn(OOCCH3)2:2H2O is dissolved in 20 ml of methanol with vigorous stirring at around 50 °C, diluted to 200 ml, and then cooled to room temperature. The medicine was put in the bottle. On top of the pre registered solution, a few drops of the special surfactant PVP are added under vigorous stirring. The zinc Acetate solution received 15 ml of 0.01 01 M NaOH in methanol, which was added drop wise while being stirred for a value. A sheet has been shown to be stable under ambient condition.

After that white ppt, transfer to a linear Teflon autoclave and heat for two days at 160°C. Following that, distilled water and ethanol were used to wash the annealed solution once again and ZnO nanoparticles were extracted by centrifugation at 1200 rpm. and dried in a vacuum oven at about 1500 d egrees Celsius. Finally, ZnO nanorod powder was collected for further processing.

c. Synthesis of ZnO nano spheres:

For the synthesis of ZnO nanospheres, use the solvothermal method described in previous section.
The only capping reagent is CTAB.

2. **Material Characterizations:**

a. X-Ray Diffraction (XRD) Analysis

In the measurement, the XRD pattern (open and spherical morphology) of ZnO nanoparticle was recorded by Bruker D 8 Xray diffractometer. CuKa radiation (λ = 0.15418 nm) is chosen in the construction of the Xray copper plane. Figure 3 presents XRD spectra of three different architures.

ISSN(Online) : 2319-8753
ISSN (Print) : 2347-6710

International Journal of Innovative Research in Science, Engineering and Technology

(An UGC Approved, High Impact Factor, Monthly, Peer Reviewed Journal) | Impact Factor: 7.089|

UGC Approval No: 48027

Vol. 6, Issue 4, April 2017

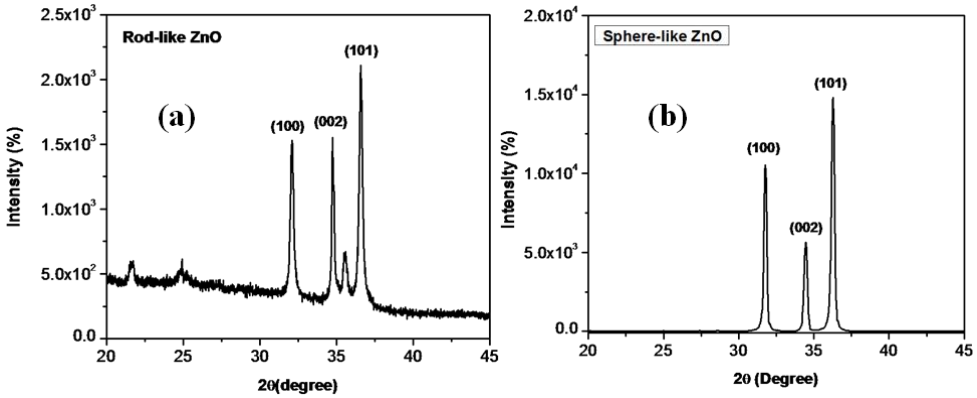

Figure 3: XRD spectra of ZnO (a) rod and (b) sphere

The recorded XRD spectra show that the main (hkl) diffraction planes of ZnO nanoparticles are at 2θ = 32, 34.6 and 36.4 degrees (100), (002) and (101). JCPDS Card No.: 36-451 [20] supports data of XRD spectra of synthetic Nanomaterials with different morphologies. It is clear from these spectra that there is no significant change in the diffraction pattern, but a significant change in correlation. For plane (002) the change in intensity is very pronounced. This may be due to their morphological development. From XRD data using Scherrer's equation, the mean size of zinc oxide rods and spherical nano particles calculated as 57 nm and 26 mm respectively.

b. Scanning Electron Microscopy Analysis

A SEM image (figure 4) shows that the morphological structure of the ZnO material. SEM images clearly shows that the shape and size of the particles. Rod and spherical materials should be given special consideration due to their nanometer size. ZnO nanorods have a hexagonal cross-section and a length that ranges from 80 to 120 nm on average. The solubility of precursors in solvents with various saturation vapour pressure affects the final growth process of early new creation of crystals nanoparticles, including the early nucleation of crystals [24, 25]. On the growth material, water-soluble surfactants like CTAB and PVP can establish coordination with Zn ions [26]. The quick development of ZnO nuclei is reserved for the low vapour pressure. Crystal growth is influenced by the surfactant CTAB and PVP's chain lengths.

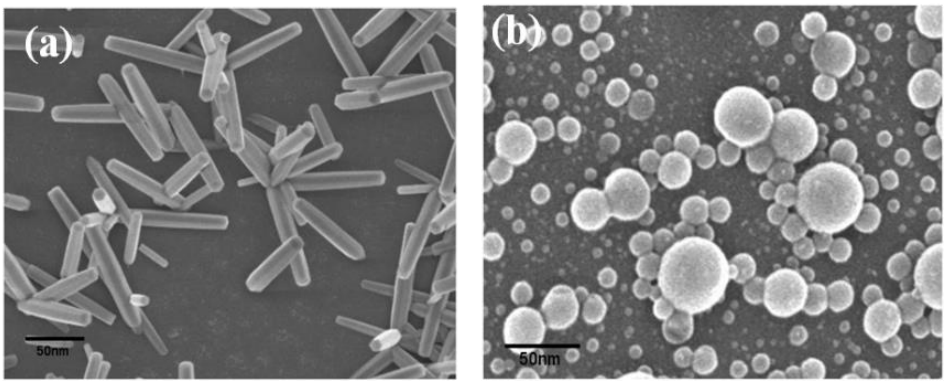

Figure 4: SEM images of ZnO (a) rod and (b) sphere

ISSN(Online) : 2319-8753
ISSN (Print) : 2347-6710

International Journal of Innovative Research in Science, Engineering and Technology

(An UGC Approved, High Impact Factor, Monthly, Peer Reviewed Journal) | Impact Factor: 7.089|

UGC Approval No: 48027

Vol. 6, Issue 4, April 2017

3. Optical Characterizations:

UV-vis Absorption Study:

The absorption of incoming photons depends on the morphology and aspect ratio of the material used. It is possible to obtain more absorption due to the different structures of the synthesized ZnO. The above UV-Vis absorption Spectra of ZnO were recorded with a 2401 PC spectrophotometer from Shimadzu. Spectra of pseudo data were recorded separately in chloroform medium 100 µL of 0.1 mM dispersion solution was taken from each ZnO. In the wavelength range of 300 to 800 nm, the absorption Spectra of ZnO nanoparticles with various morphologies were captured in the chloroform solution (figure 5). The closed spectrum is as follows:

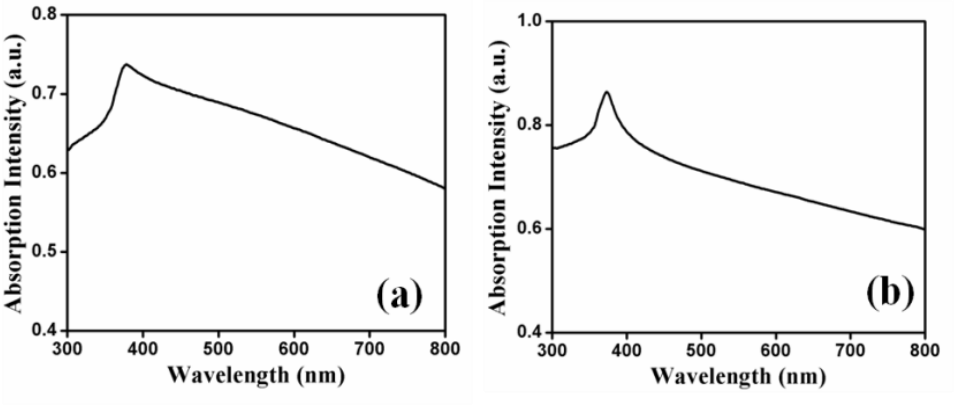

Figure 5: UV-vis absorption spectra of ZnO (a) rod and (b) sphere.

Obviously, rod-shaped nanoparticles (Figure 5(a)) show peaks at lower wavelengths, ie
higher energy. For spheres such as ZnO, the absorption maximum is shifted (redshift) to higher wavelengths. Interestin gly, all absorption is in the visible region.

Optical energy & band gap evaluation:

It is well known that zno is a General material. The direct optical band gap is roughly defind by optical absorption. To understand the synthetic properties, the absorption Coefficient was estimated from the UV-Vis data. Considering the information, for example, the direct optical band gap was estimated as 3.1 5 eV the Tauc diagram and 3 with the help of the Tauc equation. Rod and spherical morphologies are 25 ev respectively (figure 6) in the case of road like nano morphologies, the absorption is very high due to the low band gap which is explained by the high absorption. Inorganic semiconductors having large band gaps are crucial for solar application that operates at higher temperatures (compared to room temperature).

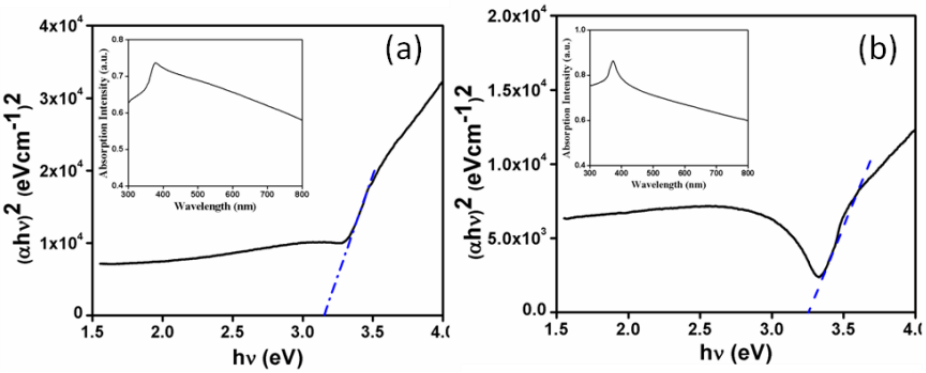

Figure 6: Tauc's plot of ZnO (a) rod and (b) sphere

ISSN(Online) : 2319-8753
ISSN (Print) : 2347-6710

International Journal of Innovative Research in Science, Engineering and Technology

(An UGC Approved, High Impact Factor, Monthly, Peer Reviewed Journal) | Impact Factor: 7.089|

UGC Approval No: 48027

Vol. 6, Issue 4, April 2017

The direct band gap energy varies significantly for spherical and rod-like objects because to morphological modifications. The abundance of states close to the conduction band during chemical development may be the cause of this. According to these optical band gap studies, the synthesized substance is a member of the bandgap semiconductor family. Due to its high absorbency, the band gap measurement further illustrates the novelness of the surfactant-guided manufacturing process of nonmaterial. ZnO nanoparticles' actual band gap is 3.3 eV, previously reported by Berger et al. 1997 [27] and 3.4 eV, Soosen Samuel M et al. [28] is very high compared t o our synthetic material. The nucleation process of the material can cause changes in the energy band gap of these materials. The organic surfactant's chain length also affects this nucleation. The electron affinity of the synthesized nonmaterial decreases as the electron density rises during chemical development, which may have an impact on the optical characteristics of semiconductors and, in turn, on the metal-semiconductor junctions. The shape of the nanomaterial affects the consistency of the interface throughout the entire device. This guarantees reliable equipment and effective transportation. We are motivated to look into the impact of material morphology on effective charge and effective interference at metal-semiconductor interfaces by this behavior (lower band gap with increasing absorption and grain size). We created spherical and rectangular ITO/ZnO/Al-based Schottky junctions for extensive examination.

4. Fabrication of Schottky diode (configuration ITO/ZnO(NP)/Al):

Previous step fabrication of Schottky diodes, the ITO coated glass surfaces were cleaned by ultrasonic technique with soap solution Acetone ethanol and finally distilled water and Dried in a vacuum oven. Dispersion solution of ZnO and nanoparticles with different molecologies in chloroform medium were prepared by ultrasonic process. After obtaining the solution, rotate the ITO coated substrates for 2 minutes at 1200 rpm, turning the coating for each difference before cleaning. Then the zno thin film was dried in a vacuum at 1000°C for 30 minutes. With the help of surface profiler, the thickness of the film was optimized to ~200Å. Aluminium was deposited in this film by thermal evaporation process to prepare the metal semiconductor interface, using the shadow image to maintain a good diode area of 7.065×10^{-2} cm.

5. Device Characterizations

A Keithley 2400 source meter connected to a computer was used to determine the current-voltage (I-V) characteristics of Schottky barrier diodes made of metal (Al) and semiconductor (ZnO nanoparticles with various morphologies). The I-V characteristic curve was used to analyze the performance, best, and peak height of diodes. The analysis of the charge carrier follows the rules of conventional semiconductor theory. Figure 7 displays the current-voltage (I-V) characteristics of ITO/ZnO/Al based Schottky diodes with various nanomaterial electrical properties. All of these characteristic curves indicate that at at ±1 **V**, the material processing ratios for spherical and rod-shaped materials are, respectively, 21.62 and 10.93.

ISSN(Online) : 2319-8753
ISSN (Print) : 2347-6710

International Journal of Innovative Research in Science, Engineering and Technology

(An UGC Approved, High Impact Factor, Monthly, Peer Reviewed Journal) | Impact Factor: 7.089|

UGC Approval No: 48027

Vol. 6, Issue 4, April 2017

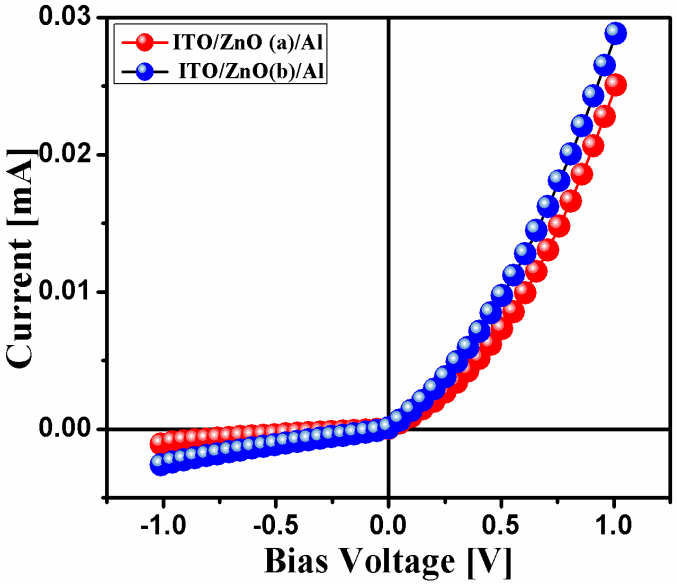

Figure 7: Current-voltage characteristics of ITO/ZnO (a)/Al and ITO/ZnO (b)/Al Schottky diodes.

Here, ZnO(a) represent spherical and ZnO(b) rod-like samples,

The characteristic current voltage curve by determining the following diode equation [29, 30]:

$$I = I_0 . exp\left(^{qV}/_{nkT}\right)\left[1 - exp\left(^{-qV}/_{kT}\right)\right]$$

$$I_0 = AA^{*}T^2 exp\left(^{-q\Phi_B}/_{kT}\right)$$

$$n = \left(^{q}/_{kT}\right)^{dv}/_{dln(I)}$$

where I_0, q, k, T, A, A*, n and Φ_B represents saturation current, electron charge, Boltzmann constant, Kelvin temperature, effective area, Richardson constant, ideality factor and barrier heights respectively. For oxide semiconductor materials, the effective diode area is calculated as$7.065x10^{-3}$ cm^2 and barrier potential height are the research on constant is calculated as The series resistance ideally factor and their potential height are determined using the Cheung equation [31]:

$$^{dv}/_{dln(I)} = \left(^{nkT}/_{q}\right) + IR_s$$

$$H(I) = V - \left(^{nkT}/_{q}\right) ln\left(^{I_0}/_{AA^{*}T^2}\right)$$

and

$$H(I) = IR_s + n\Phi_B$$

The series resistance and target values are calculated by the slope and intersection against dV/dln(I). I plot (Fig. 8) and the barrier height is estimated from interpolation against **H(I)** vs. **I** draw (Fig. 9).

ISSN(Online) : 2319-8753
ISSN (Print) : 2347-6710

International Journal of Innovative Research in Science, Engineering and Technology

(An UGC Approved, High Impact Factor, Monthly, Peer Reviewed Journal) | Impact Factor: 7.089|

UGC Approval No: 48027

Vol. 6, Issue 4, April 2017

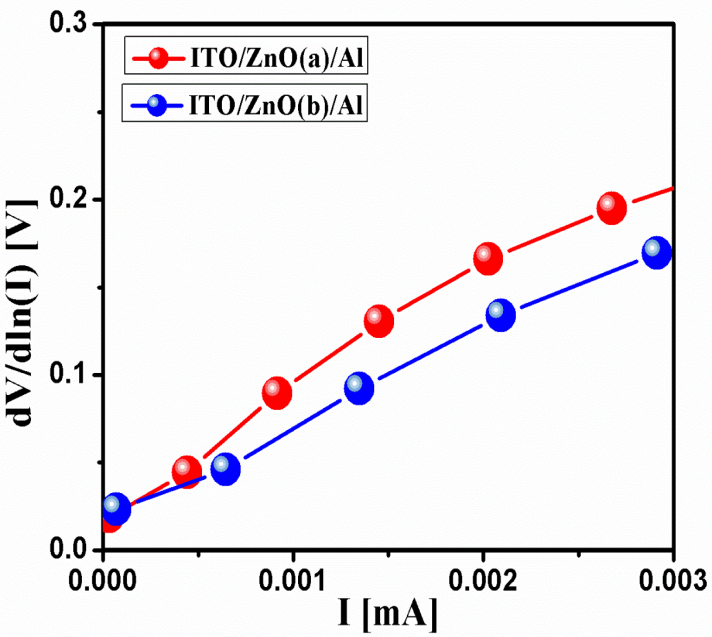

Figure 8: dV/dln(I) vs I plots of ITO/ZnO(a)/Al and ITO/ZnO(b)/Al schottky diode

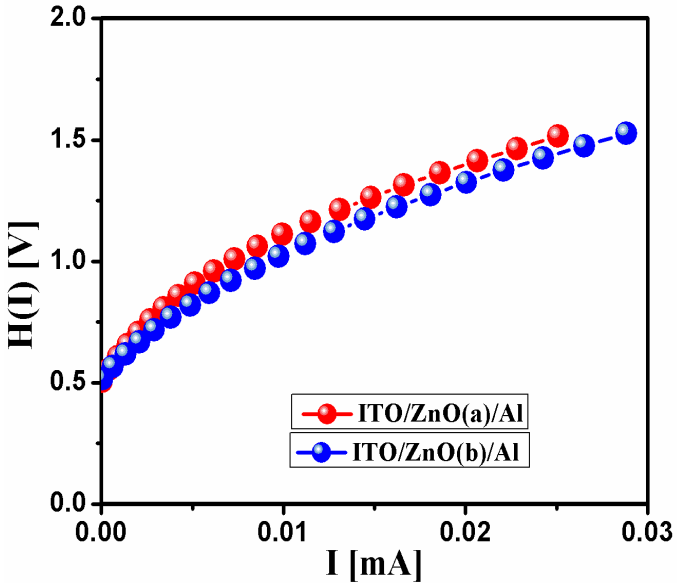

Figure 9: H(I) vs I plot of ITO/ZnO(a)/Al and ITO/ZnO(b)/Al schottky diode**.**

The height, optimum, and performance of metal (Al)-semiconductor (ZnO) junctions as determined by morphology are shown in Table 1. Positive feeling in this context is distinct from articulation that deviates from positive behavior. The presence of layers or the high likelihood of interaction between electrons and holes in the depletion zone may be to blame for this discrepancy [32]. The 1.63 and 1 features are the best.

ISSN(Online) : 2319-8753
ISSN (Print) : 2347-6710

International Journal of Innovative Research in Science, Engineering and Technology

(An UGC Approved, High Impact Factor, Monthly, Peer Reviewed Journal) | Impact Factor: 7.089|

UGC Approval No: 48027

Vol. 6, Issue 4, April 2017

Figure 85 demonstrates that the contact is not a compact metal-semiconductor but rather needs an interface layer [33], which can be brought on by environmental factors like humidity or wind direction.

Table I: Characteristic of the Schottky Diodes

Schottky Diode Configuration	On/Off current ratio	Ideality Factor (n)	Potential barrier height Φ_B (eV)	Series Resistance from dV/dln(I) vs I curve (Ω)	Series Resistance from H(I) vs I curve (Ω)
ITO/ZnO(Sphere)/Al	**21.63**	**1.63**	**0.43**	**$0.86x10^5$**	**$1.58x10^5$**
ITO/ZnO(Rod)/Al	**10.94**	**1.85**	**0.47**	**$0.62x10^5$**	**$1.15x10^5$**

ITO/ZnO (sphere)/Al and ITO/ZnO (rod)/Al Schottky diodes' barrier heights were calculated to be 0.43 eV and 0.47 eV, respectively. The high barrier potential (B) is closely correlated with the work function (M) of metals and the electron affinity (χ) of semiconductors, according to the Schottky-Mott theory [34]. Given that the fixation, i.e. In the Schottky limit, does not influence the Fermi level, the barrier height is a measurement of the difference between Φ_M and χ [35].Spheres such as ZnO based Schottky diodes have lower voltage drop
compared to rod diodes. This may be due to changes in electron affinity due to band structures and band gap energies o f semiconductor nanoparticles. This can be clarified by working quickly.This is beyond our current job. Instead, we use other techniques based on semiconductor
theory to investigate and understand the transport process in materials. ln(I) vs. The ln(V) graph (Fig. 10) shows the de nsity of the charge.

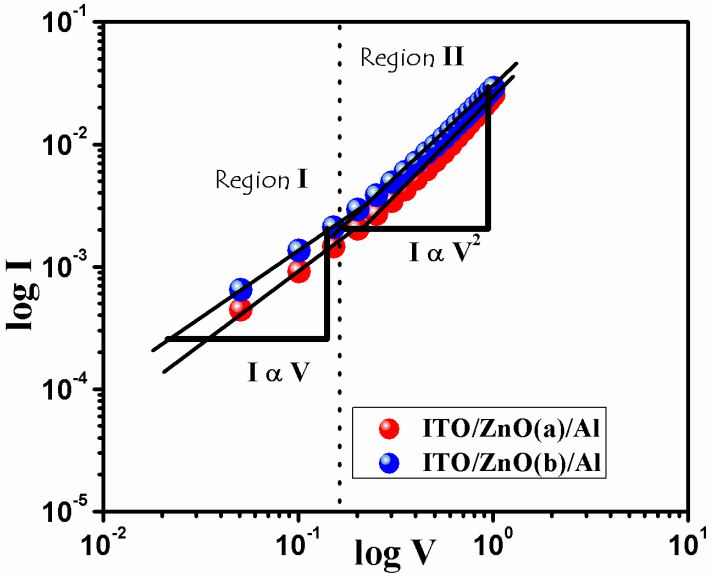

Figure 10: log(I) vs. log(V) plot of ITO/ZnO(a)/Al and ITO/ZnO(b)/Al devices

ISSN(Online) : 2319-8753
ISSN (Print) : 2347-6710

International Journal of Innovative Research in Science, Engineering and Technology

(An UGC Approved, High Impact Factor, Monthly, Peer Reviewed Journal) | Impact Factor: 7.089|

UGC Approval No: 48027

Vol. 6, Issue 4, April 2017

In this figure the –I region represents the thermionic region and the II region represents the SCLC region. ZnO(a) and ZnO(b) represents Spherical and rod like structures, respectively **(Fig.** 10). The array of logarithmic features shows two different regions with different slopes **(Fig.** 10). Zone I is experienced due to thermionic discharge, Which June II is defined due to field load Limiting current and charge reversal. The recombination rate can be calculated by interpolating with the career mobility. To better understand the coupling, the career motion of the device was estimated as $9.8x10^6$ $cm^2V^{-1}s^{-1}$ and $9.1x10^6$ $cm^2V^{-1}s^{-1}$ by measuring the slope of ln(I) versus ln(V) for region II. Space charge limiting current (SCLC) equation for setting IT O / ZnO (spheres) / Al and ITO / ZnO (rods) / Al with the help of Mott-Gurney [36]:

$$J = \frac{9\mu_{eff}\,\varepsilon_0\varepsilon_r}{8}\left(\frac{V^2}{d^3}\right)$$

Where J is the current density, ε0 is the permittivity of the free surface, and εr is the relative permittivity. A data value of εr = 2.9 was used for metal oxide semiconductor nanoparticles [37, 38]. Estimates of carrier mobility for spherical m orphologies are high, indicating very low recombination rates in devices made with these morphologies.
This may be due to the effect of rod shaped nanoparticles in the active film rather than the spherical nanoparticles[39] supported by the instruments pre-measured ideality factors. It can also be due to the thickness of the film. By optimizing the thickness of the film, the recombination rate can be further reduced, resulting in products with greater mobility and modest charge transfer phenomena.

6. Summary:

This experiment presents the hydrothermal synthesis and characterization of Spherical and rod- like ZnO nanoparticles. The band gap energy of the nanoparticles was estimated using light absorption data. Finally, we investigate the effect of nanoparticle structure on metal- semiconductor circuit diodes. The schottky diode parameters were evaluated from the current- voltage characteristics. The component charge transfer mechanism with mobility was illustrated accurately by SCLC equation for the devices.

REFERENCES

[1] W. U. Huynh, J. J. Dittmer, A. P. Alivisatos, *Science* 295 (2002) 2425
[2] A. Petrella, M. Tamborra , M. L. Curri, *Journal of Physical Chemistry B* 109 (2005) 1554
[3] C. Kligshirn, *Phys. Status Solidi. B* 71 (1975) 547
[4] H. V.Wenckstern, G. Biehne, R. A. Rahman, E. M. Kaidashev, H. Hochmuth, M. Lorenz , M. Grundmann, *Appl. Phys. Lett.* 88 (2006) 0921020
[5] U. Grossner, S. Gabrielsen, T. M. Borseth, J. Grillenberger, A. Y. Kuznetsov, B. G. Svensson, *Appl. Phys. Lett.* 85 (2004) 259
[6] M. W. Allen, M. M. Alkaisi, S M Durbin, *Appl. Phys. Lett.* 89 **(**2006) 1035201
[7] N. Saito, H. Haneda, T. Sekiguchi, N. Ohashi, I. Sakaguchi, K. Koumoto, *Adv. Mater.* 14 (2002) 418
[8] S. Liang, H. Sheng, Y. Liu, Z. Huo, Y. Lu, H. Shen, *J. Cryst. Growth* 225 (2001) 110
[9] S. P. Singh, S. K. Arya, P. Pandey, B.D. Malhotra, S. Saha, K. Sreenivas , V. Gupta, *Appl. Phys. Lett.* 91 (2007) 063901
[10] J. Mescher, N. Christ, S. Kettlitz, A. Colsmann, U. Lemmer, *Appl. Phys. Lett.* 101 (2012) 073301
[11] V. A. L. Roy, A. B. Djurisic,W. K. Chan, J. Cao, H. F. Lui and C. Surya, *Appl. Phys. Lett.* 83 (2003) 141
[12] Q. H. Chen, W. G. Zhang, *J. Non-cryst. Solids* 353 (2007) 374
[13] W. J. E. Beek, M. M. Wienk, A. Rene, J. Janssen, *Adv. Mater.* 16 (2004)
[14] S. V. Bhat, A. Govindaraj, C. N. R. Rao, *Solar Energy Materials and Solar Cell*, 95 (2011) 2318
[15] Y. Chen, D.M. Bagnall, H. Koh, K. Park, K. Hiraga, Z. Zhu, T. Yao, *J. Appl. Phys.* 84 (1998) 3912
[16] C. Ton-That, M. R. Philips and T.P Nguyen, *Journal of Luminescence* 128 (2008) 2031
[17] Y. Abdollahi, A. H. Abdullah1, Z. Zainal and N. A. Yusof, *International Journal of Basic & Applied Sciences* 11(4) (2011) 62

ISSN(Online) : 2319-8753
ISSN (Print) : 2347-6710

International Journal of Innovative Research in Science, Engineering and Technology

(An UGC Approved, High Impact Factor, Monthly, Peer Reviewed Journal) | Impact Factor: 7.089|

UGC Approval No: 48027

Vol. 6, Issue 4, April 2017

[18] S. Liang, H. Sheng, Y. Liu, Z. Huo, Y. Lui and H. Shen, *J. Cryst. Growth* 225 (2001) 110
[19] A. Y. Polyakov, N. B. Smirnov, E. A. Kozhukhova, V. I. Vdovin, K. Ip, Y. W. Heo, D. P. Norton and S. J. Pearton, *Appl. Phys. Lett.* 83 (2003) 1575
[20] G. Yuan, Z. Ye, L. Zhu, J. Huang, Q. Qian, B. Zhao, *J. Cryst. Growth* 268 (2004) 169
[21] H. V. Wenckstern, E. M. Kaidashev, M. Lorenz, H. Hochmuth, G. Biehne, J. Lenzner, V. Gottschalch, R. Pickenkain, M. Grundmann, *Appl. Phys. Lett.* 84 (2004) 79
[22] K. Ip, B. P. Gila, H. Onstine, E. S. Lambers, Y. W. Heo, K. H. Baik, D. P. Norton, S. J. Pearton, S. Kim, J. R. LaRoche, F. Ren, *Appl. Phys. Lett.* 84 (2004) 5133
[23] K. Ip, Y. W. Heo, K. H. Baik, D. P. Norton, S. J. Pearton, S. Kim, J. R. LaRoche, F. Ren, *Appl. Phys. Lett.* 84 (2004) 2835
[24] J. Zhang, *Chem. Mater*. 14 (2002) 4172
[25] X. Gao, X. Li, W. Yu, *J. Solid State Chem.* 178 (2005) 1139
[26] H. Zhang, D. Yang, D. Li, X. Ma, S. Li, D. Que, *Cryst. Growth Des.* 5 (2005) 547
[27] L. I. Berger, Semiconductor Materials, CRC Press, Boca Raton, FL (1997) 801
[28] M. S. Samuel, L. Bose, K.C. George, *Academic Review* 16 (2009) 57
[29] S. M. Sze, Physics of semiconductor devices, New York, Wiley, 1979
[30] E. H. Rhoderick, R. H. Williams, Metal–semiconductor contact, 2nd ed. Clarendon, Oxford (1988)
[31] S. K Cheung, N. W. Cheung, *Appl. Phys. Lett*. 49 (1986) 85
[32] M. Campos, L. O. S. Bulhoes, C. A. Lindino, *Sens. Actuators* 87 (2000) 67
[33] F. Yakuphanoglu, *J. Phys. Chem. C*, 111 (2007) 1505
[34] W. Schottky, *Naturwissenschaften* 26 (1938) 843
[35] N. F. Mott, *Proc. Cambridge Philos. Soc.* 34 (1938) 568
[36] P. W. M. Blom, M. J. M. de Jong, M. G. van Munster, *Phys. Rev. B: Condens. Matter.* 55 (1997) 656
[37] M. Schidleja, C. Melzer, H. von Seggern, *Adv. Mater*. 21 (2009) 1172
[38] J. S. Park, J. M. Lee, S. K. Hwang, S. H. Lee, H. J. Lee, B. R. Lee, H. Park, J. S. Kim, S. Yoo, M. H. Song and S. O. Kim, *J. Mater. Chem.* 22 (2012) 12695
[39] J. Sworakowski, J. Ulanski, *Annu. Rep. Prog. Chem. Sect.C* 99 (2003) 87